Dendrochronologia 74 (2022) 125979

Contents lists available at ScienceDirect

Dendrochronologia

journal homepage: www.elsevier.com/locate/dendro

Tree-ring isotopes from *Araucaria araucana* as useful proxies for climate reconstructions

Tiphaine Penchenat [a,*], Valérie Daux [a], Ignacio Mundo [b,c], Monique Pierre [a], Michel Stievenard [a], Ana Srur [b], Laia Andreu-Hayles [d,e,f], Ricardo Villalba [b]

[a] *Laboratoire des sciences du climat et de l'environnement (LSCE), Université Paris-Saclay, CNRS, CEA, UVSQ, Orme de Merisiers, 91191 Gif-sur-Yvette, France*
[b] *Instituto Argentino de Nivología, Glaciología y Ciencias Ambientales (IANIGLA), CONICET, Av. Ruiz Leal s/n Parque General San Martín, Mendoza, Argentina*
[c] *Facultad de Ciencias Exactas y Naturales, Universidad Nacional de Cuyo, Padre Contreras 1300, Mendoza, Argentina*
[d] *Tree-Ring Laboratory, Lamont-Doherty Earth Observatory of Columbia University, 61 Route 9 W, Palisades, NY 10964, USA*
[e] *CREAF, Bellaterra (Cerdanyola del Vall.s), Barcelona, Spain*
[f] *ICREA, Pg. Lluís Companys 23, Barcelona, Spain*

ARTICLE INFO

Keywords:
Araucaria araucana
$\delta^{13}C$
$\delta^{18}O$
Tree-ring width
Carbohydrates

ABSTRACT

Tree-ring width (TRW) chronologies have been widely and long-time used to reconstruct past climate variations in the Andes in South America. The use of tree-ring isotopic chronologies is still not widespread in this region although they have proved to be very efficient climate proxies. *Araucaria araucana* (Molina) K. Koch is a conifer tree species with some multi-century-old individuals that offers an excellent opportunity to measure stable carbon ($\delta^{13}C$) and oxygen ($\delta^{18}O$) isotopes in cellulose from long tree-ring records. Here, we explore whether current or stored carbohydrates are used for *A. araucana* radial growth and we assess the potential of a tree-ring isotopic record of to study past climate variability. Eleven *A. araucana* cores from a dry and high-elevation forest at the northern border of Patagonia, Argentina (38°55'S, 70°44'W) were selected for stable isotopes analyses. The strong correlation between the isotopic composition of the first and second parts of the same ring, but also the strong relationships between $\delta^{13}C$ and $\delta^{18}O$ records with climate parameters of the current growing season such as temperature, show that tree-rings are built mostly with carbohydrates produced during the current growing season with little or no supply from storage or reserves. This finding leads to reconsidering the interpretation of the legacy effect (i.e. ecological memory effects) based on the previously described strong negative correlation between *A. araucana* TRW chronologies and previous growing season temperature and suggests a dependence of radial tree growth on the level of development of organs. Regarding climate sensitivity, the *A. araucana* tree-ring $\delta^{13}C$ chronology is strongly related to current summer temperature ($r = 0.82$, $p < 0.001$), vapour pressure deficit (VPD; $r = 0.79$, $p < 0.001$), precipitation ($r = -0.53$, $p < 0.001$) and SPEI2 ($r = -0.73$, $p < 0.001$). These strong relationships support the use of $\delta^{13}C$ of *A. araucana* tree-ring cellulose to reconstruct past temperature variations at regional scale in relation with large-atmospheric drivers of climate variability such as the Southern Annular Mode. The *A. araucana* tree-ring $\delta^{18}O$ chronology is also correlated with temperature ($r = 0.42$, $p < 0.01$) and VPD ($r = 0.45$, $p < 0.01$) of the winter preceding the growing season. This suggests that trees are using water from precipitation infiltrated in the soil during the previous recharge period (autumn-winter). The weak correlations of $\delta^{18}O$ with current summer atmospheric conditions and the decoupling between $\delta^{18}O$ and $\delta^{13}C$, may be due to a high rate of oxygen exchange between sugars and xylem water (P_{ex}) during cellulose synthesis, which dampens evaporative isotopic fractionation.

* Correspondence to: Université Paris-Saclay, CNRS, CEA, UVSQ, Laboratoire des sciences du climat et de l'environnement, Orme des Merisiers, 91191 Gif-sur-Yvette, France.

E-mail addresses: tiphaine.penchenat@lsce.ipsl.fr (T. Penchenat), valerie.daux@lsce.ipsl.fr (V. Daux), iamundo@mendoza-conicet.gob.ar (I. Mundo), monique.pierre@lsce.ipsl.fr (M. Pierre), michel.stievenard@lsce.ipsl.fr (M. Stievenard), asrur@mendoza-conicet.gob.ar (A. Srur), lah@ldeo.columbia.edu (L. Andreu-Hayles), ricardo@mendoza-conicet.gob.ar (R. Villalba).

https://doi.org/10.1016/j.dendro.2022.125979
Received 22 October 2021; Received in revised form 13 April 2022; Accepted 6 June 2022
Available online 10 June 2022

1. Introduction

Tree-rings have made an important contribution to our understanding of climatic variations over the last centuries and millennia in the Andes (Boninsegna et al., 2009; Villalba et al., 2003). Climate-sensitive *Polylepis tarapacana* in the Altiplano in South America provide the highest-elevation tree-ring chronologies worldwide spanning for centuries to millennia (Morales et al., 2012). Even closer to the Equator at 11ºS, but with shorter time span, *Polylepis rodolfo-vasquezii* have also shown climate sensitivity, in particular with growing season temperature (Requena-Rojas et al., 2020). Further south in the Central Andes in Chile (32°S - 36°S), centennial oscillations in precipitation were inferred from millennium-long records of *Austrocedrus chilensis* (Le Quesne et al., 2006, among others). Tree-ring records have also provided substantial insight into regional temperature and precipitation variations in northern Patagonia from recent centuries to the last millennium. Millennium-long chronologies from *Fitzroya cupressoides* have been used to reconstruct past temperature variations on both sides of the Northern Patagonian Andes (Lara et al., 2020, among others), while precipitation variability in this region have largely been based on moisture-sensitive *Araucaria araucana* - *A. chilensis* chronologies (Boninsegna et al., 2009 and references therein, Hadad et al., 2021).

During the past two decades, several studies have measured stable carbon and oxygen isotopic composition in tree-ring cellulose ($\delta^{13}C$ and $\delta^{18}O$ respectively) from various tree species in the South American Andes such as *Nothofagus pumilio* (Grießinger et al., 2018; Lavergne et al., 2017a, 2017b, 2016; Tognetti et al., 2014), *Nothofagus betuloides* (Meier, 2019), *A. chilensis* (Roig et al., 2006), *F. cupressoides* (Lavergne et al., 2018, 2017a, 2016; Urrutia-Jalabert et al., 2015c), *P. tarapacana* (Rodriguez-Caton et al., 2021), *A. araucana* (Arco Molina et al., 2019). These isotopic records exhibited significant correlations with local climate and/or hemispheric patterns of climate variability such as the Southern Annular Mode and ENSO. These strong links indicate that $\delta^{18}O$ and $\delta^{13}C$ chronologies are useful tools for reconstructing past climate and environmental conditions, as well as past atmospheric dynamics in the South America sector of the Southern Hemisphere.

The carbon and oxygen data have also been used to determine if the tree-ring cellulose was originated from current or stored carbohydrates (Kimak and Leuenberger, 2015; Kress et al., 2009). The remobilization of stored carbohydrates is frequently observed in deciduous trees, in particular during the formation of earlywood (Helle and Schleser, 2004). Although they do not generally rely on reserves for initiating their growth, evergreen species can also show a strong carbon carry-over effect (*Pinus kesiya* and *Pinus armandii*; Fu et al., 2017). When tree-rings are formed with both remobilized stored material and current assimilates, the tree-ring cellulose $\delta^{18}O$ and $\delta^{13}C$ usually hold complex and mixed information about the environmental conditions during the current growing season and previous periods of carbohydrates production (Helle and Schleser, 2004; Kagawa et al., 2006). Therefore, it is essential to determine the origin of the carbohydrates used for growth prior to undergoing isotope-based climate reconstructions.

To our knowledge, only two studies conducted on *A. araucana* have included tree-ring stable isotopes as diagnostic tools. $\delta^{13}C$ was used, indeed, to estimate the evolution of intrinsic water use efficiency (iWUE) and evaluate the physiological response of this species to climate change and the increase in atmospheric CO_2 concentrations by Arco Molina et al. (2019). Recently, Puchi et al. (2021) studied *A. araucana* stands in Northern Patagonia and showed that tree-ring isotopes and anatomical traits could be combined to identify stands at risk of drought-induced dieback.

The present study was conducted in northwestern Patagonia where trees from a dry and high-elevation forest were targeted to study the use of current assimilation carbon or stored carbohydrates in *A. araucana,* as well as the potential of their $\delta^{18}O$ and $\delta^{13}C$ tree-rings as climate proxies. Specifically, we first determined the origin (current or prior year) of carbohydrates used for tree radial growth by analyzing the influence of previous and current year conditions on the isotopic signature in the cellulose and measuring intra-ring variations. Second, we compared the conclusions derived from the isotopes with those drawn from the growth patterns and proposed an integrative explanation for apparently incompatible findings. Finally, we debated on the strength of the climate signal and the spatial representativeness of the relationships between tree-ring isotopic compositions and climate parameters. Thus, we tested whether the use of C and O isotope ratios could provide new climatic information in addition to that recorded by the conventional dendroclimatic approach based on tree-ring widths.

2. Materials and Methods

A.araucana is an emblematic tree in the northern Patagonian forest from Argentina and Chile, encompassing a latitudinal three-degree range from 37°20'S to 40°20'S approximately (Veblen et al., 1995). In Argentina, *A. araucana* is confined along the Andes mountains between 38°40'S and 39°20'S in the province of Neuquén. *A. araucana* is adapted to highly contrasting environments growing from very humid (4000 mm/year at some Chilean sites) to dry environments (e.g. ~500 mm/year) (Veblen, 1982; Veblen et al., 1995). It forms monospecific stands, but it is often associated with *Nothofagus antarctica* and *N. pumilio*, mostly on south-facing slopes at elevations between 1000 and 1400 m a.s.l. (Veblen et al., 1995). Mixed stands with *A. chilensis*, *Lomatia hirsuta* and other shrub species are recorded at ecotonal environments with the Patagonian steppe in the eastern distribution sector (Burns, 1991, 1993).

2.1. Tree species and study site

Trees from *A. araucana* were sampled at Sainuco, a site located in a dry and high-elevation location for the species, and supposedly sensitive area in the northwestern of Patagonia. The Sainuco sampling site (SAI, 38°55'S, 70°44'W) is located at 1660 m a.s.l elevation on a southeast-facing slope at the northern portion of the Sierra de Catán Lil, 57 km east of the main Andes divide (Fig. 1a). The soil is from the Andisol order (del Valle, 1998). At Sainuco, *A. araucana* forms a monospecific, open stand (Fig. 1b), mostly composed by mature individuals with a density of about 100 trees per hectare. The lack of young trees is likely due to cattle feeding on fallen seeds (Burns, 1991). The annual mean temperature and total precipitation at Sainuco are 8.4 ± 0.4 °C and 516 ± 94 mm, respectively, over the period 1974–2014 (See Meteorological data section; CRU TS 4.03 database, Harris et al., 2020). Regarding climate seasonality, lower temperatures occurred from May to August when most of the precipitation is received (Fig. 1c).

2.2. Sample collection and preparation

Cores from *A. araucana* at the Sainuco site were taken in November 2015 and processed at the Instituto Argentino de Nivología, Glaciología y Ciencias Ambientales (IANIGLA CONICET), Mendoza, Argentina. Initially used for ring width dendrochronological analyses, cores were mounted and sanded following Stokes and Smiley (1968), visually crossdated using the Yamaguchi (1991) approach. Ring widths were measured to the nearest 0.001 mm, and the computer program COFECHA (Holmes, 1983) was used to detect measurement and dating errors. The individual tree-ring width timeseries were computed to generate a regional *A. araucana* ring width chronology. Regarding the calendar dating, as in the Southern Hemisphere the growing season straddles two calendar years each annual ring was assigned to the year in which ring formation started following the Schulman's convention (1956). The transition from the previous to the current biological year takes place between April and September, i.e. mid fall to early spring.

The oldest 10 trees, with ages ranging between 240 and 546 years old were selected for the isotopic analyses. At the Laboratoire des Sciences du Climat et de l'Environnement (LSCE, Gif-sur-Yvette, France), the

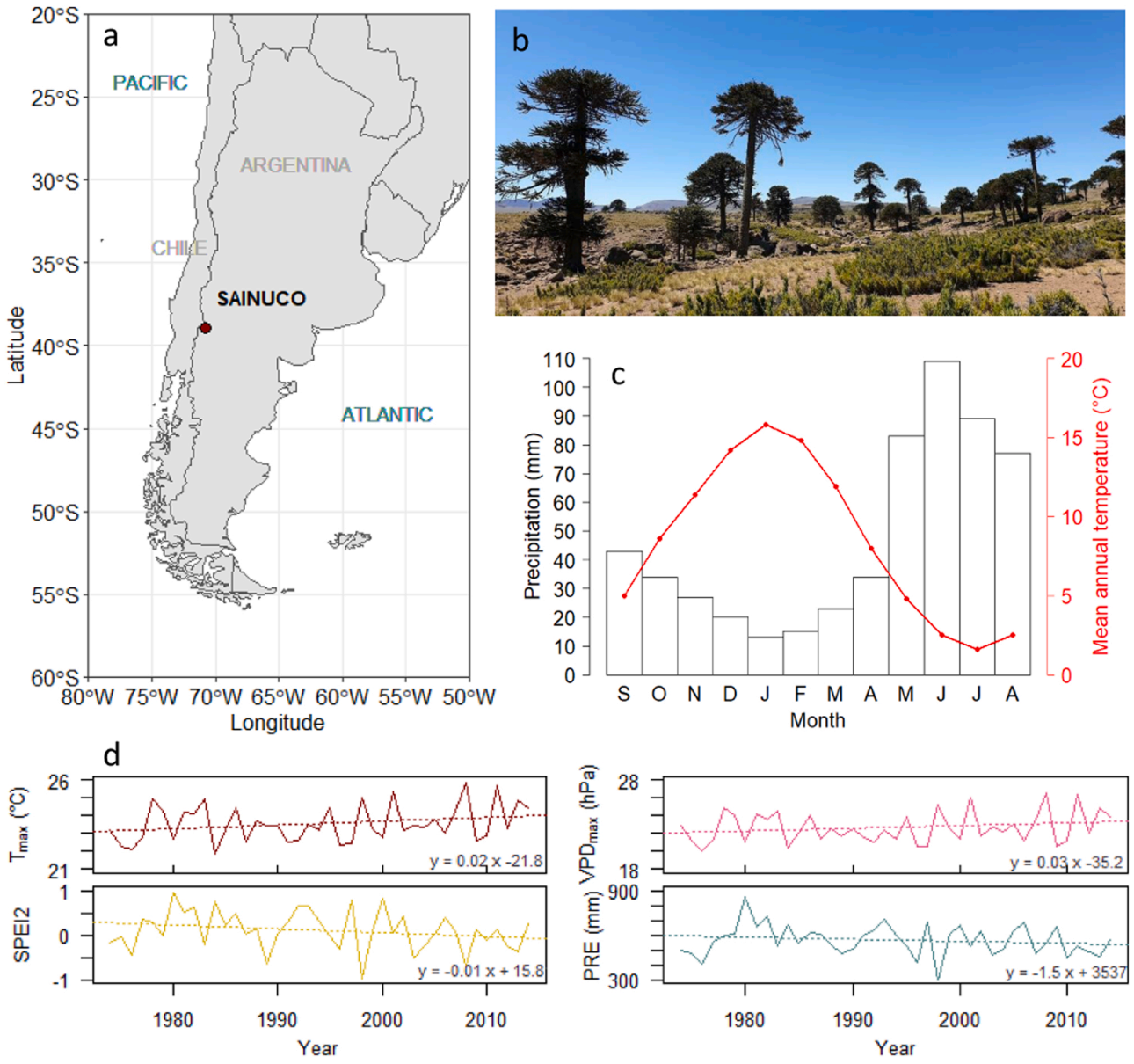

Fig. 1. a) Location of the Sainuco site in western Argentina. b) Picture of the Sainuco site. c) Umbrothermal diagram of monthly mean temperature and total precipitation data from September to August between 1974 and 2014. d) Climate data from 1974 to 2014 for maximum temperature (T_{max}) and vapour pressure deficit (VPD_{max}) averaged from December to January, and yearly Standardised Precipitation-Evapotranspiration Index 2 (SPEI2) and precipitation (PRE, $p > 0.05$). The dotted lines represent the linear trends for the data; their equations and the significance of the slope (p-value) are provided.

mounted cores were peeled off using hot water and dried for several hours at ambient air. For each core, forty-one annual rings (1974–2014) were split using a scalpel, and the α-cellulose was extracted from the wood of each ring sample following the chemical procedure described by Leavitt and Danzer (1993). In order to quantify the intra-ring variability of the isotopic compositions of oxygen and carbon, an additional core (named 'intra-core' hereafter) with wide rings was selected and earlywood and latewood were cut and analyzed separately over the 1950–2014 period. Since the transition from earlywood to latewood in *A. araucana* tree-rings is very gradual and consequently difficult to situate unambiguously, we divided the rings into two parts: the first portion corresponding to the first three quarters of the ring (F3/4) and the second portion to the last fourth (L1/4), as shown in Fig. 2. Therefore, the wood did not strictly correspond to early- and latewood but nevertheless reflected successive phases during the growth period. These parts were weighted, processed and analyzed in the same way as the complete rings of the other 10 samples. The L1/4 sample of 1998 was lost during cellulose extraction due to very small amount of wood.

2.3. Measurement of carbon and oxygen isotopes in tree-rings

The isotopic compositions of oxygen and carbon of tree-ring cellulose were simultaneously obtained by high temperature pyrolysis (HTP) in a high temperature conversion elemental analyzer (TC-EA, Thermo Scientific) coupled to a mass spectrometer (IRMS, IsoPrime). To correct for potential instrumental drifts, a cellulose standard (Whatmann © CC31) was analysed every three samples in each sequence of analysis. The analytical precisions of the instrument were within 0.20‰ and 0.10‰ for oxygen and carbon, respectively, based on the standard uncertainty of the mean. HTP was shown to be a suitable and reliable proceeding for the determination of the isotopic composition of carbon in cellulose simultaneously during the analysis of oxygen ratios. Although an isotope effect related to the non-statistical conversion of the organic carbon to CO may alter the results for carbon (Knöller et al., 2005), we prevented

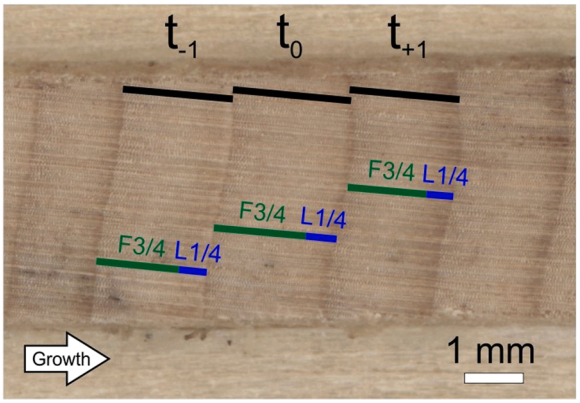

Fig. 2. Sub-division of the rings into the F3/4 and L1/4 portions on a 5-mm diameter *A. araucana* core. Growth direction is indicated by the white arrow and scale bar is presented on the low-right corner.

this issue by adjusting the results from the HTP using a combustion-pyrolysis regression previously obtained with pairs of measurements as proposed in Woodley et al. (2012). Therefore, the adjusted carbon values were equivalent to the values that would have been obtained using combustion.

The oxygen and carbon isotopic compositions were expressed as δ ($\delta^{13}C$ for carbon and $\delta^{18}O$ for oxygen), in per mill (‰):

$$\delta = (R_{cell}/R_{STD} - 1) \times 1000 \quad (1)$$

where R_{cell} is the oxygen isotope ratio (^{18}O /^{16}O) of cellulose referring to R_{STD}, the Vienna Standard Mean Ocean Water (Coplen, 1996), or the carbon isotope ratio ($^{13}C/^{12}C$) of cellulose referring to R_{STD}, the Vienna Pee-Dee Belemnite (Coplen, 1996).

The $\delta^{13}C$ records show a decreasing trend over time due to the decrease in $\delta^{13}C$ of atmospheric CO_2 since the beginning of industrialization. Therefore, the measured $\delta^{13}C$ were corrected for this anthropogenic isotopic effect using the standard $\delta^{13}C$ correction model from Dombrosky (2020). Hereafter, the physiological and (paleo-)climatic interpretations were made on the basis of these corrected $\delta^{13}C$ values.

2.4. Chronology development

The individual $\delta^{18}O$ and $\delta^{13}C$ series were averaged to generate isotopic site chronologies, hereafter $\delta^{18}O_{SAI}$ and $\delta^{13}C_{SAI}$ chronologies (data in Supplementary Material).

Several descriptive statistics were calculated to assess the coherence between individual series and the final quality of the chronologies: r (Pearson correlation coefficient), CI (Confidence Intervals), RBAR (mean Pearson correlation coefficient among tree-ring series within a chronology; Briffa, 1995) and EPS (Expressed Population Signals; Wigley et al., 1984). EPS enables to assess how well a mean chronology based on a finite number of series represents the hypothetical perfect chronology consisting of an infinite number of series (Wigley et al., 1984). CI was calculated for each year according to the following equation:

$$CI = t \times \left(SD \Big/ \sqrt{N}\right) \quad (2)$$

Where SD is the standard deviation, N is the number of individual series and t is the two-tailed Students' t value at 95% confidence.

2.5. Meteorological data

We used the climate data (1973 and 2015) from the two nearest grid points to our sampling site taken from CRU TS 4.03 gridded database (70.75°W - 38.75°S and 70.75°W - 39.25°S; Harris et al., 2020; https://crudata.uea.ac.uk/cru/data/hrg/). From these gridded points regional monthly maximum and minimum temperatures (T_{max}, T_{min} in °C), precipitation (PRE, in mm) and actual vapour pressure (AVP, in hPa) were retrieved. The monthly vapour pressure deficit (VPD_{max}) was calculated as the difference between the monthly saturated vapour pressure (SVP_{max}) and the AVP. SVP_{max} was calculated with the Teten (1930)'s equation:

$$SVP = 6.108 \times \exp(17.27 \times T/237.3 + T) \quad (3)$$

Where T is T_{max} in Celsius degree, and SVP is in kPa.

VPD_{mean} was calculated using SVP_{mean} (average of SVP_{max} and SVP_{min}). Its variations are very similar to those of VPD_{max} (correlation coefficient of 0.97). For coherency with T_{max}, VPD_{max} is used and discussed in this paper.

We also extracted the Standardized Precipitation-Evapotranspiration Index (SPEI), to compare our results with a drought index (Vicente-Serrano et al., 2010; https://spei.csic.es/), and the monthly photosynthetically active radiation flux (PAR, in W/m^2) from the NASA/GEWEX Surface Radiation Budget Release 3.0 dataset (https://asdc.larc.nasa.gov/project/SRB). We present in this paper the most significant results which were obtained with SPEI calculated on a two-month timescale (SPEI2). From ERA5 (ECMWF's fifth generation atmospheric global climate reanalysis covering the period January 1950 to the present; Hersbach et al., 2020; https://cds.climate.copernicus.eu/cdsapp#!/dataset/reanalysis-era5-single-levels-monthly-means?tab=form), we extracted atmospheric maximum temperature at 2 m above ground level (T2m, in K) and surface pressure 850 mb (SLP, in Pa). We also used the Southern Annular Mode (SAM) index from ERA5 (difference between slp40 and slp65) because the SAM is the main mode of climate variability at high latitudes in the Southern Hemisphere (Garreaud et al., 2013).

Spatial correlation patterns between the Sainuco isotopic chronologies and T_{max}, SPEI2, PRE, T2m and SLP 850 mb were obtained for the interval 1974–2014 using the KNMI Climate Explorer web application (https://climexp.knmi.nl/).

3. Results

The RBAR and EPS values for the $\delta^{13}C$ series were 0.22 and 0.74, respectively. For the $\delta^{18}O$ series, these statistics were equal to 0.54 and 0.92, which shows a greater shared variance among the $\delta^{18}O$ individual series (Fig. 3). For 10 trees, the CI were 0.49‰ and 0.66‰ for $\delta^{13}C_{SAI}$ chronology and $\delta^{18}O_{SAI}$ chronology respectively. Over 1974–2014, for the $\delta^{13}C_{SAI}$ and $\delta^{18}O_{SAI}$ chronologies, the average and standard deviations (SD) were -20.09 ± 0.69‰ and 30.44 ± 0.94‰, respectively, and the trends were both positive (+0.002 and +0.015‰), but not significant at 95% confidence level. The one-lag autocorrelation coefficients were 0.20 (non-significant (ns), $n = 41$) and 0.31 ($p < 0.05$, $n = 41$) for carbon and oxygen respectively, indicating that $\delta^{18}O_{SAI}$ was slightly more affected by past physiological and/or environmental conditions than $\delta^{13}C_{SAI}$. The $\delta^{13}C_{SAI}$ and $\delta^{18}O_{SAI}$ chronologies were not significantly correlated to one another ($r = -0.23$, ns, $n = 41$).

Over 1950–2014, the $\delta^{13}C$ chronologies obtained for F3/4 ($\delta^{13}C_{F3/4}$) and L1/4 ($\delta^{13}C_{L1/4}$) showed slightly positive, but non-significant trends (Fig. 4), and were positively and strongly correlated with each other ($r = 0.71$, $p < 0.001$, $n = 64$; Fig. 5). The correlation coefficient between $\delta^{13}C_{SAI}$ and $\delta^{13}C_{F3/4}$ ($r = 0.51$, $p < 0.001$, $n = 41$) was larger than between $\delta^{13}C_{SAI}$ and $\delta^{13}C_{L1/4}$ ($r = 0.46$, $p < 0.01$, $n = 40$). The isotopic composition of the whole rings, hereafter $\delta^{13}C_{WR}$, was calculated as the sum of $\delta^{13}C_{F3/4}$ and $\delta^{13}C_{L1/4}$, weighted by the mass of cellulose chemically extracted from the F3/4 and L1/4. The correlation coefficient between $\delta^{13}C_{WR}$ and $\delta^{13}C_{SAI}$ was 0.52 ($p < 0.001$, $n = 40$), which equals the mean value of the correlation coefficients between the individual $\delta^{13}C$ series and $\delta^{13}C_{SAI}$.

The two $\delta^{18}O$ series obtained for F3/4 ($\delta^{18}O_{F3/4}$) and L1/4 ($\delta^{18}O_{L1/4}$)

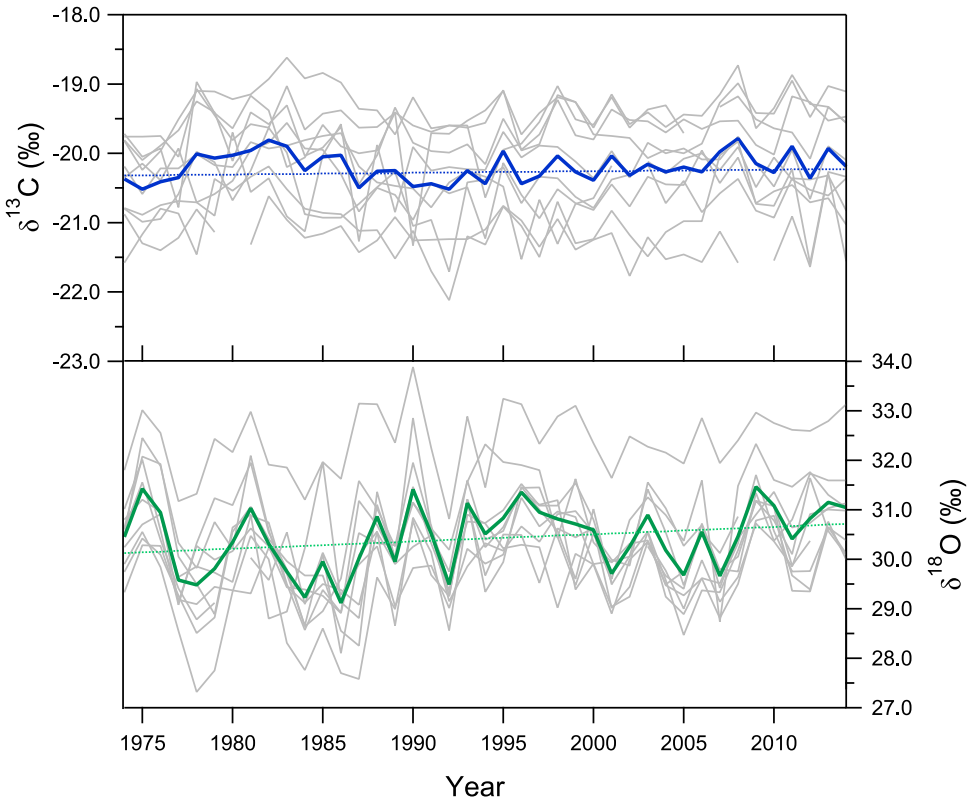

Fig. 3. Annual variations of $\delta^{13}C$ individual series (grey), $\delta^{13}C_{SAI}$ (blue) (upper graph) and $\delta^{18}O$ series (grey) and $\delta^{18}O_{SAI}$ (green) (lower graph) from 1974 to 2014. The blue and green dotted lines represent the linear trends for $\delta^{13}C_{SAI}$ and $\delta^{18}O_{SAI}$.

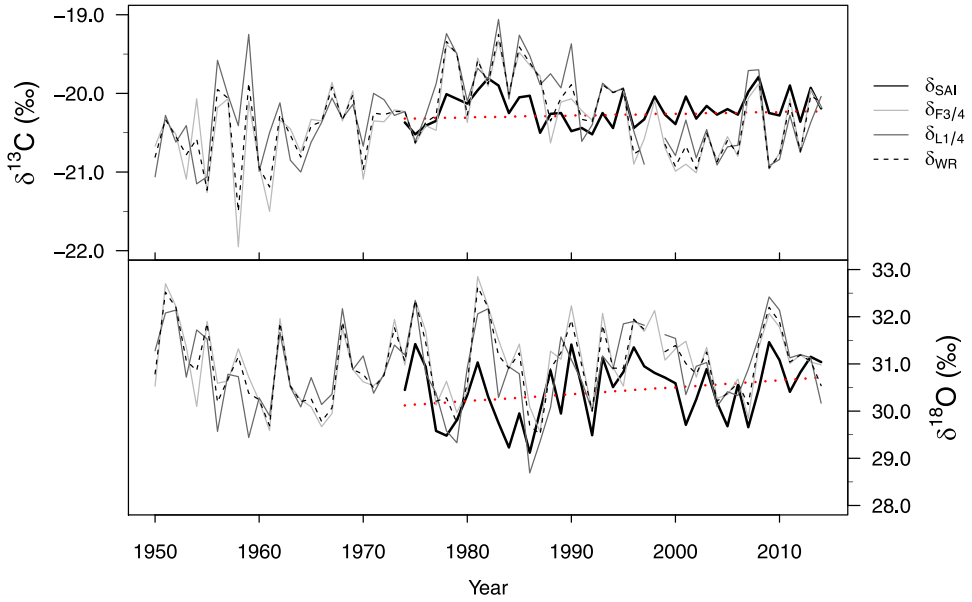

Fig. 4. Upper graph, annual variations of $\delta^{13}C_{SAI}$ (solid black line) from 1974 to 2014, $\delta^{13}C_{F3/4}$ (solid light grey line), $\delta^{13}C_{L1/4}$ (solid dark grey line) and $\delta^{13}C_{WR}$ (dot-dashed black line) from 1950 to 2014. Lower graph, annual variations of $\delta^{18}O_{SAI}$ (solid black line) from 1974 to 2014, $\delta^{18}O_{F3/4}$ (solid dark grey line), $\delta^{18}O_{L1/4}$ (solid light grey line) and $\delta^{18}O_{WR}$ (dot-dashed black line) from 1950 to 2014. The red dotted lines represent the linear trends for $\delta^{13}C_{SAI}$ and $\delta^{18}O_{SAI}$.

showed also slightly positive trends, but not-significant (Fig. 4). The correlation between $\delta^{18}O_{F3/4}$ and $\delta^{18}O_{L1/4}$ was the same as the one between $\delta^{13}C_{F3/4}$ and $\delta^{13}C_{L1/4}$ ($r = 0.70$, $p < 0.001$, $n = 64$). The correlation between $\delta^{18}O_{SAI}$ and $\delta^{18}O_{F3/4}$ ($r = 0.68$, $p < 0.001$, $n = 41$) was similar to the correlation between $\delta^{18}O_{SAI}$ and $\delta^{18}O_{L1/4}$ ($r = 0.65$, $p < 0.001$, $n = 40$; Fig. 5). The isotopic composition of the whole rings, hereafter $\delta^{18}O_{WR}$, was calculated as the sum of $\delta^{18}O_{F3/4}$ and $\delta^{13}O_{L1/4}$, weighted by the mass of cellulose chemically extracted from the F3/4 and L1/4. The correlation coefficient obtained between $\delta^{18}O_{WR}$ and $\delta^{18}O_{SAI}$ was 0.71 ($p < 0.001$, $n = 40$). Interannual variations in the $\delta^{13}C$ and $\delta^{18}O$ of F3/4 and L1/4 were consistent with those of the average Sainuco chronologies (Fig. 4).

The correlation coefficient of current year $\delta^{13}C_{F3/4}$ with current year $\delta^{13}C_{L1/4}$ ($r = 0.71$, $p < 0.001$, $n = 64$) was higher than with previous

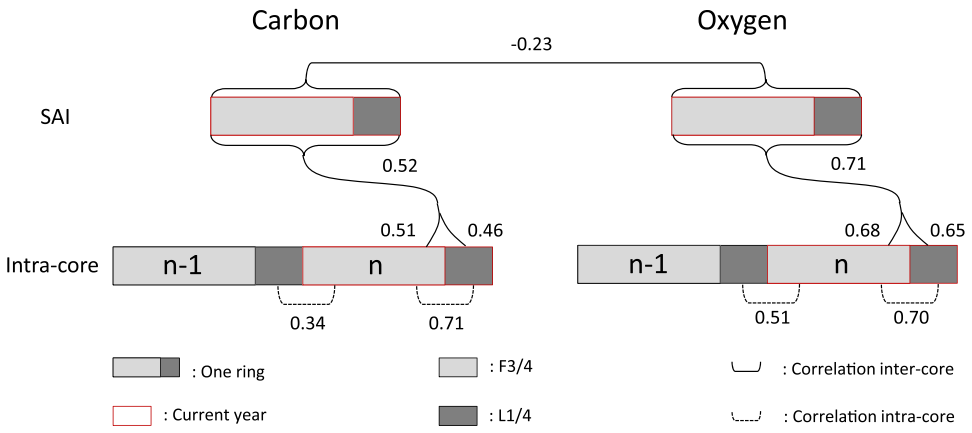

Fig. 5. Sketch of the relationships based on correlation coefficients (r) among the intra-core isotopic timeseries (F3/4, L1/4, lower panel), as well as between the intra-core timeseries and the isotopic value for the Sainuco site chronologies ($\delta^{18}O_{SAI}$ and $\delta^{13}C_{SAI}$, upper panel). n is the current year and n-1 the previous year.

year $\delta^{13}C_{L1/4}$ ($r = 0.34$, $p < 0.01$, $n = 64$, Fig. 5). Similarly, the correlation of current year $\delta^{18}O_{F3/4}$ with current year $\delta^{18}O_{L1/4}$ ($r = 0.70$, $p < 0.001$, $n = 64$) was higher than with previous year $\delta^{18}O_{L1/4}$ ($r = 0.51$, $p < 0.001$, $n = 64$).

Using linear regressions, we assessed trends in T_{max}, VPD_{max}, SPEI2 and PRE from 1974 to 2014. We found an increasing trend in T_{max} particularly during December-January (+0.9 °C, i.e. around +0.2 °C per decade) and VPD_{max} (+1.2 hPa, i.e. +0.3 hPa per decade) for the same period, and consistent decreasing ones in SPEI2 and PRE (−60 mm in annual average, i.e. −15 mm per decade) (Fig. 1d).

Correlation analyses were performed between $\delta^{13}C_{SAI}$ and $\delta^{18}O_{SAI}$ and the climate data. The monthly correlations of $\delta^{13}C_{SAI}$ and $\delta^{18}O_{SAI}$ with T_{max}, VPD_{max}, SPEI2 and PRE are shown in Fig. 6. The most significant relationship between $\delta^{13}C_{SAI}$ and climate was with December-January T_{max} of the current growing season ($r = 0.82$, $p < 0.001$, $n = 41$; Fig. 7). There was also a significant positive correlation between $\delta^{13}C_{SAI}$ and VPD_{max} over the same period ($r = 0.79$, $p < 0.001$, $n = 41$; Fig. 7), consistently with the fact that T_{max} is involved in the calculation of VPD_{max}. We also recorded a significant negative correlation between $\delta^{13}C_{SAI}$ and January SPEI2 (i.e. calculated over December-January) during the current growing season ($r = -0.73$, $p < 0.001$, $n = 41$; Fig. 7). A negative correlation was evidenced between $\delta^{13}C_{SAI}$ and December PRE of the current growing season ($r = -0.53$, $p < 0.001$, $n = 41$). A positive correlation was found between $\delta^{13}C_{SAI}$ and SAM in November-December of the current growing season ($r = 0.39$, $p < 0.05$, $n = 41$). $\delta^{18}O_{SAI}$ did not show significant relationships with any monthly meteorological data from current or previous growing seasons. In contrast, it was positively related to T_{max} (May-June; $r = 0.42$, $p < 0.01$, $n = 41$) and VPD_{max} (June-August; $r = 0.45$, $p < 0.01$, $n = 41$) of autumn-winter of the preceding growing season.

Spatial correlation analyses were conducted between the $\delta^{13}C_{SAI}$ and the mean December-January T_{max} (Fig. 8a), January SPEI2 (Fig. 8b) and December PRE (Fig. 8c) across the region from 30°S to 57°S and from 78°W to 60°W. Significant correlations were observed over a large area in the southern South America, positive with T_{max} and negative with SPEI2 and PRE. This is consistent with previous results based on monthly correlations (see above). At a larger scale from 20°N – 80°S and from 160°E – 30°W, December-January T2m from the ERA5 reanalyses (Fig. 8d) was also significantly correlated with the $\delta^{13}C_{SAI}$ record and positively over the Southern tip of the South American continent and in

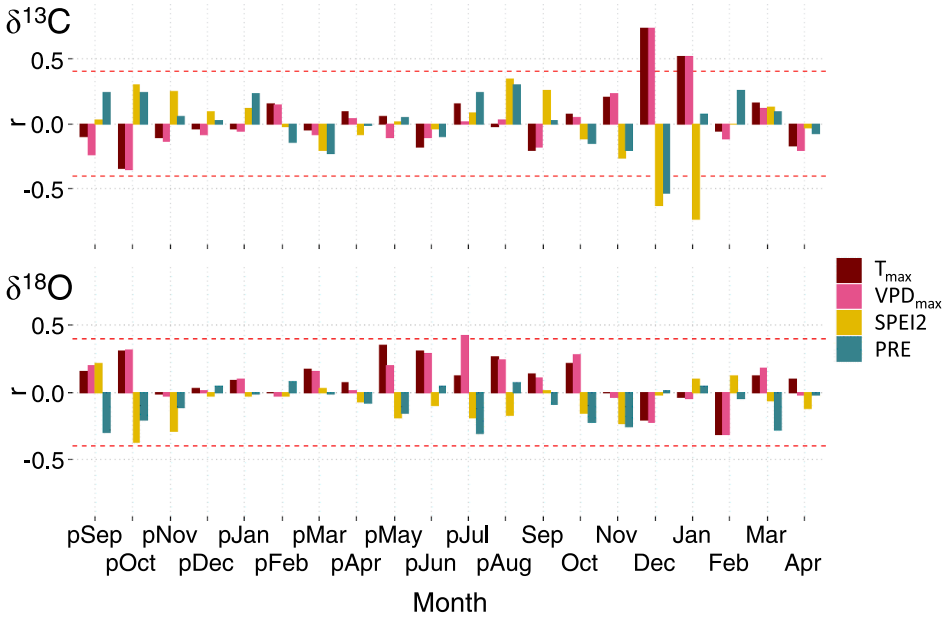

Fig. 6. Correlation coefficients between the $\delta^{13}C_{SAI}$ and $\delta^{18}O_{SAI}$ chronologies and regional monthly maximum temperature (T_{max}), maximum vapor pressure deficit (VPD_{max}), Standardized Precipitation-Evapotranspiration Index 2 (SPEI2) and Precipitation (PRE) from September of the previous growing season (pSep) to April of the current growing season (Apr) from 1974 to 2014. Red dashed lines represent the 99% confidence limits.

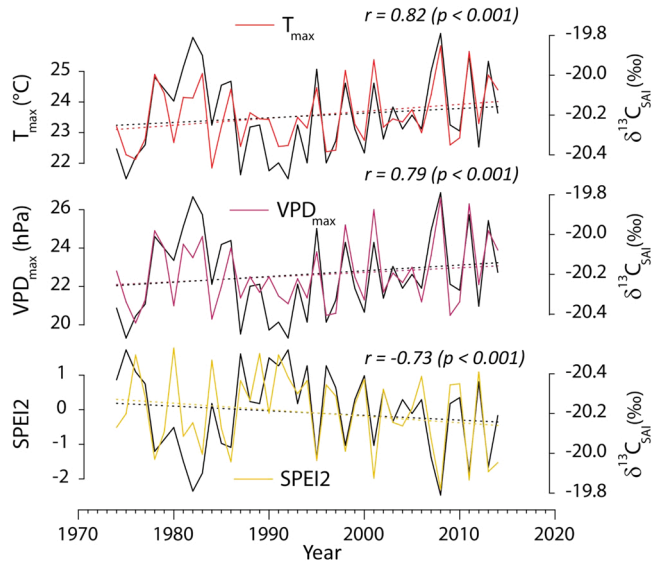

Fig. 7. Comparisons of temporal variations in *A. araucana* $\delta^{13}C_{SAI}$ (solid black line) at Sainuco, northern Patagonia with (upper) regional mean (December-January) maximum temperature (T_{max}), (middle) mean (December-January) maximum vapor pressure deficit (VPD_{max}) and (bottom) January Standardized Precipitation-Evapotranspiration Index (SPEI2, calculated over December-January corresponding to January) over the common interval 1974–2014 (41 years). To facilitate the comparison with SPEI2, the $\delta^{13}C_{SAI}$ variations are shown inverted. The correlation coefficients between records are also indicated.

the Pacific around 80°W, and negatively between 50°S and 60°S in the Pacific around 120°W and on the West Antarctic coasts (Bellingshausen and Amundsen seas). The spatial correlation between $\delta^{13}C_{SAI}$ and December SLP exhibits a similar pattern in December (Fig. 8e).

4. Discussion

4.1. Which carbohydrates is the cellulose of A. araucana rings built with?

In *A. araucana,* latewood represents about 10–22% of the ring (Falcon-Lang, 2000), but the transition between early and latewood is gradual (Díaz-Vaz, 1984; Tortorelli, 1956) and the precise separation of the two tissues is problematic. Therefore, in order to determine the intra-annual isotopic signature, the cutting at the third fourth of each ring, in order to generate F3/4 and L1/4 series approximately informs about the earlywood and latewood sections, respectively. The strong link between the isotopic records of the first and second parts of the rings ($r = 0.7$ for both $\delta^{13}C$ and $\delta^{18}O$) suggests that the two portions were formed from sugars synthesized in the same growing season. Due to the thinness of the rings, this intra-core experiment was conducted on one core only (having above average wide rings). The conclusion drawn above must therefore be taken with caution and should be ideally supported by similar tests on other trees. However, the significant correlations between $\delta^{13}C_{F3/4}$, $\delta^{13}C_{F1/4}$, $\delta^{13}C_{WR}$ ($\delta^{18}O_{F3/4}$, $\delta^{18}O_{F1/4}$, $\delta^{18}O_{WR}$) with the $\delta^{13}C_{SAI}$ ($\delta^{18}O_{SAI}$) demonstrate that the core selected for intra-annual analyses exhibited an intra-ring isotopic pattern very likely shared by the other trees of the same stand.

The positive relationships between $\delta^{13}C_{SAI}$ and climate parameters of the current growing season also suggest that the *A. araucana* tree-rings in the Sainuco site are mostly formed with current carbohydrates with little use of the previous year reserves for early season wood formation. Evergreen trees can form xylem cells in early spring using carbohydrates produced by 'old' needles grown in previous years, and from old and new needles afterwards (Barbour et al., 2002; Dickmann and Kozlowski, 1970; Glerum, 1980; Rathgeber, 2020). They are less dependent on their reserves to start their growth than deciduous species and therefore less likely to use them (Kozlowski, 1992). The evidence presented above indicates that *A. araucana* trees from Sainuco likely do not rely on stored carbohydrates for the onset of the growing season. They thus fit the pattern most commonly observed among evergreen trees. Note that these findings cannot be extrapolated to all *A. araucana* populations. Indeed, as already stressed, the intra-ring results being obtained on one single tree cannot be generalised. In addition, in a general way, the photosynthates (current or stored) selected for early growth may not only depend on the species, but also on the environment. The influence of environmental conditions can be illustrated with a study of two populations of *F. cupressoides* growing on both sides of the Andes. Different possible use of reserves in the two populations were pointed out based on significant correlations between $\delta^{13}C_{SAI}$ and previous and current summer temperature in the Chilean wet stands (Urrutia-Jalabert et al., 2015c), while only current summer temperature was significant in the Argentinian drier sites (Lavergne et al., 2017a). More studies are needed to elucidate if the humidity site conditions can be the most important factor determining the use of carbohydrates during the current or previous year.

Importantly, as tree-ring cellulose seems to be mostly formed with current photosynthates, the isotopic signal, which thus represents essentially the environmental conditions of the current growing season, can be extracted without the need for conducing intra-annual cuts in the tree-ring samples.

4.2. Does the functioning of A. araucana based on isotopic chronologies agree with that derived from tree-ring widths?

The regional tree-ring width (TRW) reference chronology for the Argentinean network of *A. araucana* sites (Mundo et al., 2012) is negatively correlated with summer temperature from the previous growing season (TRW versus T_{DJF}: $r = -0.50$, $p < 0.001$, $n = 41$), and to a lesser extent, with the current season temperature ($r = -0.32$, $p < 0.05$, $n = 0.41$). These dependencies are consistent with the inverse and one-year lagged relationships between the TRW of *A. araucana* and summer temperatures evidenced in several Patagonian sites (Hadad et al., 2014; Hadad and Roig, 2016; Muñoz et al., 2013; Villalba, 1995), a pattern which emerges with most of the gymnosperms in Northern Patagonia (Lara et al., 2020; Lavergne, 2016; Villalba, 1990; Villalba et al., 1998, 1996).

In terms of growth, the performance of trees may depend, at least partially, on reserves made the previous years. It may also rely on structures from the past (needles, buds, roots, sapwood) which may be several-year old and carry some information on conditions of the periods when they were built (Zweifel and Sterck, 2018). Indeed, as described hereafter, these past structures may be the sites where hormones essential for xylem cell formation are produced (Buttò et al., 2020). Xylogenesis can be divided into several steps, including cell enlargement, which is the most important for radial growth. This step is regulated by phytohormones (notably auxin indole-3-acetic acid; IAA; Taiz and Zeiger, 2002), produced in the primordia and young developing leaves, roots or seeds (Brumos et al., 2018; Davies, 2010; Ljung et al., 2005; Zhao, 2010). The limitation of the formation of young developing leaves and fine roots leads to a weaker hormone production whose action is necessary for radial growth (Dünser and Kleine-Vehn, 2015; Majda and Robert, 2018; Scheuring et al., 2016). This internal regulation may explain the correlation between TRW and the climatic conditions of the previous year that affect hormone production sites. As osmotic pressure is the driving force behind cell enlargement (Cuny and Rathgeber, 2014), the rate of increase in cell size depends on the water status of the tree, which is itself determined by the physical conditions of the air and soil. The correlations between TRW and the climatic conditions of the current year (Mundo et al., 2012) likely reflect this dependence.

Our results show that TRW, proxy of xylogenesis, and $\delta^{13}C_{SAI}$, proxy of assimilations (see Rodriguez-Caton et al., 2021), are controlled by

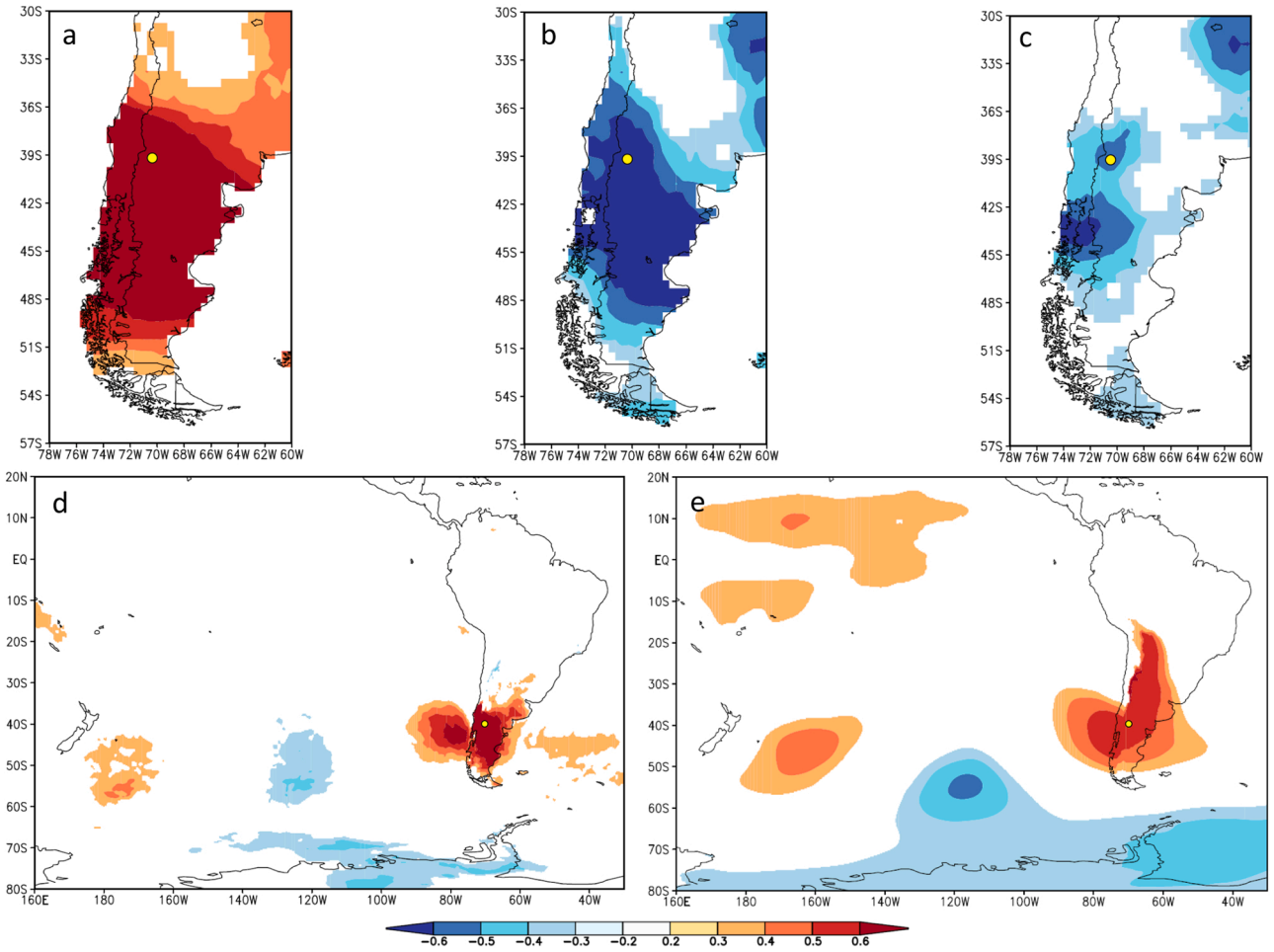

Fig. 8. Field correlation maps over 1974–2014 between the $\delta^{13}C_{SAI}$ chronology (yellow dot) and a) December-January T_{max} in, b) January SPEI2 c) December PRE, d) December-January T2m and e) in December SLP 850 mb.

different climate conditions. While the regional TRW chronology shows that the radial growth is controlled mainly by the previous summer temperature, the $\delta^{13}C_{SAI}$ indicates that the cellulose is mostly derived from current carbohydrates with very limited or even no use of reserves. These two facts can be reconciled if we consider that the legacy effect, which induces a lagged-correlation between TRW and temperature, is not due to the direct use of reserves for growth, but linked to the development of organs formed in the past, controlling the production of IAA growth hormone (Buttò et al., 2020). The correlation of $\delta^{13}C$ with current conditions reflects the fact that the majority of biomass, including cellulose, is contained in secondary cell walls formed during the second step of xylogenesis (Rathgeber et al., 2016; Zhong and Ye, 2009), very likely with current year carbohydrates in the case of *A. araucana*.

Both the regional TRW and the $\delta^{13}C_{SAI}$ records are good proxies for temperature reconstruction but the correlation between $\delta^{13}C_{SAI}$ and the meteorological parameter is the strongest (−0.5 versus 0.8 for temperature), possibly because of the absence of legacy effects on the carbon signature. A stronger relation with climate over the calibration period (1974–2014) likely leads to more accurate reconstructions by application of the transfer functions (i.e. equations linking $\delta^{13}C_{SAI}$ with climate signals, Appendix A). This advantage favors the use of $\delta^{13}C_{SAI}$ over TRW for reconstructing past temperature or other strongly related parameters like VPD_{max}.

4.3. Why are the C and O isotopic compositions in A. araucana tree-rings related to climate?

Consistently with rings formed with current season photosynthates, the $\delta^{13}C_{SAI}$ and $\delta^{18}O_{SAI}$ are strongly related to several climate parameters along the current year. In the following lines we develop the possible physiological mechanism behind these patterns.

The strong relationship between $\delta^{13}C_{SAI}$ and current summer VPD_{max} (December-January, $r = 0.79$) is likely due to the control of stomatal conductance at the leaf level by VPD_{max}. Indeed, trees adjust the opening of their stomata according to VPD_{max} and try to avoid as much as possible critical water tension in their xylem network (Running, 1976). Stomatal conductance not only regulates water loss but also the flux of CO_2 from the outside air to the substomatal cavity. Therefore, together with the activity of the Rubisco enzyme, stomatal conductance controls CO_2 concentration in the substomatal cavity, which in turn, controls carbon discrimination in C3 plants. The larger the VPD_{max}, the lower the CO_2 substomatal concentration and the carbon isotope discrimination. The VPD_{max} influence may also work through the evaporation of water from the surficial layers of the soil, affecting tree water status and, thus, stomatal conductance (Grossiord et al., 2020).

The $\delta^{13}C_{SAI}$ is also strongly related to the summer T_{max} (December-January, $r = 0.82$). The temperature signal in $\delta^{13}C_{SAI}$ may reflect the influence of temperature on VPD_{max} and in turn, of this variable on stomatal conductance. Indeed, as expressed in Eq. 3, SVP increases exponentially with temperature. As AVP does not generally increase at the same rate as temperature, warmer conditions induce increased

VPD_{max}, and decreased carbon isotope discrimination. The discrimination is also affected by the activity of the Rubisco enzyme. The more active the enzyme, the greater the carbon removal from the sub-stomatal cavity and the lower the isotopic discrimination. In C3 plants, the rate of photosynthesis does not depend much on temperature under current atmospheric conditions (Berry and Bjorkman, 1980). However, the catalytic activity of Rubisco decreases (increases) under conditions of low (high) light intensity (Mott and Woodrow, 2000). PAR correlates positively with summer T_{max} (December-January, $r = 0.55$, $p < 0.01$, $n = 25$; not shown). Thus, the $\delta^{13}C_{SAI}$-temperature link may be reinforced by the light-regulated activity of Rubisco. The dependence of $\delta^{13}C_{SAI}$ on temperature reflects a chain of causality rather than a direct effect of temperature on stomatal conductance and Rubisco activity.

The negative relations of $\delta^{13}C_{SAI}$ with PRE (December, $r = -0.53$) and SPEI2 (January, $r = -0.73$) during the growing season may be indirect and result from the dependence of these meteorological parameters on air saturation with water. Indeed, the higher the VPD_{max}, the less likely is water condensation and therefore precipitation, but the higher is SPEI2 ($r = 0.80$, $p < 0.001$, $n = 41$ between PRE and SPEI2 in December-January). $\delta^{13}C_{SAI}$ may also be related to summer PRE through the effect of soil water content on stomatal conductance. However, the low December PRE is unlikely to contribute significantly to soil moisture, and the relationship between PRE (from December or yearly) and soil moisture can be complex. Only soil moisture monitoring could help clarifying the relation between $\delta^{13}C_{SAI}$ and PRE.

The $\delta^{18}O_{SAI}$ is positively correlated with T_{max} (May-June, $r = 0.42$) and VPD_{max} (June-August, $r = 0.45$) of the late autumn and winter before the growing season. The $\delta^{18}O$ in soil water, which trees tap from, depends on the history of the air masses that provide moisture, including rainout driven by temperature variations, and evaporation at soil level (Sprenger et al., 2016). The pumping of water occurs without isotopic fractionation (Bariac et al., 1990; Dawson and Ehleringer, 1993; Rothfuss and Javaux, 2017). At the leaf level, evaporative fractionation, a temperature-dependent process, induces the isotopic enrichment of leaf water and the subsequent sugars (Cernusak et al., 2016; Gonfiantini et al., 1965). Although exchanges between organic oxygen and xylem water oxygen occur during cellulose synthesis, the isotopic composition of cellulose, which derives from that of sugars, also presents an enriched character (e.g. Barbour and Farquhar, 2004). Thus, the relation of $\delta^{18}O_{SAI}$ with T_{max} reflects the role of temperature in rainout history and/or in evaporative fractionation. The fact that the highest relation between $\delta^{18}O_{SAI}$ and temperature was found during the austral winter before the growing season suggests that the $\delta^{18}O_{SAI}$ likely depends more on the winter $\delta^{18}O_{precipitation}$ than on summer evaporative fractionation. The dependence on winter $\delta^{18}O_{precipitation}$ makes sense as winter is the rainy season and very probably the water recharge period in the soil. The link between $\delta^{18}O_{F3/4}$ and the previous-year $\delta^{18}O_{L1/4}$, the significant autocorrelation at 1-year lag of $\delta^{18}O_{SAI}$ ($r = 0.31$, $p < 0.05$), and the dependence of $\delta^{18}O_{SAI}$ on climate parameters of the autumn-winter preceding the growing season, do not contradict the conclusion drawn with $\delta^{13}C_{SAI}$ on the use for growth of the current sugars. Indeed, in seasonally dry environments like Sainuco, trees may rely largely on tightly bound pore water infiltrated during the previous recharge period (autumn-winter) for their water supply during the dry growing season (Brooks et al., 2009). Unfortunately, there are no $\delta^{18}O_{precipitation}$ records long enough available in the region to be compared with our $\delta^{18}O_{SAI}$ data.

In dry environments, trees tend to close their stomata to avoid losing water excessively and being at risk of embolism. The low $\delta^{18}O$ sensitivity to summer VPD observed at Sainuco could thus reflect a strong reduction of stomatal conductance in response to low soil moisture. However, this conclusion is not in agreement with the results obtained with carbon which are not in favor of stomatal closure but rather of a modulation of the stomatal conductance (by VPD). Cheesman and Cernusak (2016) compared leaf and trunk $\delta^{18}O_{cellulose}$ in trees along an aridity gradient. They found that leaf $\delta^{18}O_{cellulose}$ demonstrated a strong climatic signal all along the gradient whereas trunk $\delta^{18}O_{cellulose}$ was not influenced by summer variables at dry sites. They explained the decoupling between leaf and trunk isotopic composition by an increase, with decreasing humidity, of the rate of oxygen exchange between sugars and xylem water (P_{ex}) during cellulose synthesis. Szejner et al. (2020) also evidenced experimentally an enhancement of the proportion of the oxygen exchanged between sugars and source water with decreasing relative humidity. At the dry Sainuco site, the lack of significant relations between current climate variables and $\delta^{18}O_{SAI}$ may be ascribed to a high P_{ex} reinforcing the source signal and dampening the climate signal.

The combined analysis of carbon and oxygen isotope compositions can be used to clarify the interpretation of carbon discrimination assuming that a positive correlation between the two ratios reflect a regulation of $\delta^{13}C_{SAI}$ by stomatal conductance rather than rubisco activity (Roden and Farquhar, 2012; Scheidegger et al., 2000). However, this dual-isotope approach is fully valid if the $\delta^{18}O$ of the source water of the trees is constant. As the variations of $\delta^{18}O_{SAI}$ here seem to mirror those of the source, possibly because P_{ex} has a high value, the dual-isotope approach is not applicable.

The $\delta^{13}C_{SAI}$ captured variations in summer temperature, precipitation and SPEI2 over a large area of Patagonia, south of ≈ 33°S (Fig. 8a, b and c). Yet, these different climate parameters are mainly influenced by the SAM (Garreaud et al., 2013, 2009; Garreaud and Aceituno, 2007; Villalba et al., 2012). This mode of variability describes the north-south movements of westerly winds and is related to pressure anomalies between mid and high-latitudes in the Southern Hemisphere. In its negative phase, the wind belt moves equatorward bringing cold and wet air masses to mid-latitudes of the South American continent. In its positive phase, the belt moves southward, and the mid and high-latitudes of South America face high pressure, warmth and low humidity. At Sainuco latitude, SAM therefore exerts some control on temperature, pressure and humidity. The correlation between $\delta^{13}C$ at Sainuco and the SAM index are rather low, probably because $\delta^{13}C_{SAI}$ is influenced by a variety of factors, including local effects. However, the spatial correlations of $\delta^{13}C_{SAI}$ with temperature at 2 m and high pressure on a hemispheric scale show the characteristic annular SAM pattern (Fig. 8d and e). Our results are in line with those of Lavergne et al. (2017a) who found a positive and significant correlation between $\delta^{13}C$ and December-February SAM.

At mid-latitudes, temperature variations may not only be influenced by the SAM, but also by the El Niño–Southern Oscillation (ENSO) located at lower latitudes in the Pacific Ocean (Garreaud et al., 2009). During normal meteorological conditions in the South Pacific, the trade winds drive the warm surface waters westward. During an El Niño event, warm surface waters flow back eastward due to weakening trade winds promoting higher surface water temperatures along the South American coast. So, the influence of ENSO on regional climate in South America can be assessed through the analysis of the correlations between proxy records and sea surface temperature (SST) in the equatorial Pacific. Here, we found no significant association between $\delta^{13}C_{SAI}$ and SST indicating that the influence of ENSO on climate in the study area is weak or masked by local effects.

5. Conclusions and perspectives

Variations in tree-ring width of *A. araucana* trees fit well into a broad spatial pattern of negative correlations with summer temperature. Radial growth of *A. araucana* is controlled in the first order by thermometric conditions in the previous year. Our results show that the carbon of the rings is mostly assimilated during the current growing season, which indicates that growth is not directly mediated by the accumulation of reserves. We thus hypothesize that temperature in year n-1 influences growth during year n by affecting the development of organs (needles, roots, etc.) where growth hormones are produced.

$\delta^{13}C_{SAI}$ is strongly linked to several climatic parameters of the current summer. In particular, it has an exceptionally strong correlation

with temperature. This dependence results from the indirect effect of temperature on stomatal conductance (via VPD_{max}), possibly reinforced by the effect of insolation (correlated to temperature) on enzymatic activity. The strong $\delta^{13}C_{SAI}$-temperature correlation makes possible and promising the use of the cellulose $\delta^{13}C$ from *A. araucana* tree-rings at Sainuco to reconstruct past temperature variations in this poorly documented area of Northern Patagonia. The variations of $\delta^{13}C_{SAI}$ and summer temperature, which is under the influence of the SAM, are consistent over large areas of southern South America. This pattern confirms the interest of $\delta^{13}C_{SAI}$ for understanding past climate on a regional scale.

Variations in tree-ring $\delta^{18}O_{SAI}$ appear to be controlled primarily by variations in source $\delta^{18}O$, possibly because the rate of oxygen isotopic exchange between source water and sugars during cellulose synthesis is high. This assumption could be reinforced by comparing the isotopic composition of the *A. araucana* tree-rings with the $\delta^{18}O$ in precipitation simulated by climate models. A better understanding of the causes of variation of $\delta^{18}O_{SAI}$ may thus lead to the possibility of tracing the origin of air masses in relation to the modes of climate variability.

Declaration of Competing Interest

The authors declare the following financial interests/personal relationships which may be considered as potential competing interests: Valerie Daux reports financial support was provided by BNP-PARIBAS 'Climate Initiative' program. Laia Andreu-Hayles reports financial support was provided by NSF projects AGS 1903687 and AGS-1702789.

Acknowledgments

Funding: This work was supported by the project THEMES from the BNP-PARIBAS foundation. T.P. was supported by a 'Phare' PhD fellowship from the Commissariat à l'Energie Atomique, France. RV has been partially supported by the Consejo Nacional de Investigaciones Científicas y Técnicas and the Ministerio de Ciencia, Tecnología e Innovación, Argentina (PICT 2018-03691). LAH was funded by the National Science Foundation, USA (AGS-1903687 and AGS-1702789).

Appendix A. Supporting information

Supplementary data associated with this article can be found in the online version at doi:10.1016/j.dendro.2022.125979.

References

Arco Molina, J.G., Helle, G., Hadad A., R.F., M.A., 2019. Variations in the intrinsic water-use efficiency of north Patagonian forests under a present climate change scenario: tree age, site conditions and long-term environmental effects. Tree Physiol. 00, 1–18. https://doi.org/10.1093/treephys/tpy144.

Barbour, M.M., Farquhar, G.D., 2004. Do pathways of water movement and leaf anatomical dimensions allow development of gradients in H2O18 between veins and the sites of evaporation within leaves ? Plant. Cell Environ. 27, 107–121. https://doi.org/10.1046/j.0016-8025.2003.01132.x.

Barbour, M.M., Walcroft, A.S., Farquhar, G.D., 2002. Seasonal variation in δ13C and δ18O of cellulose from growth rings of Pinus radiata. Plant, Cell Environ. 25, 1483–1499. https://doi.org/10.1046/j.0016-8025.2002.00931.x.

Bariac, T., Klamecki, A., Jusserand, C., Létolle, R., 1990. Evolution de la composition isotopique de l'eau (18O) dans le continuum sol-plante-atmosphere. Geochim. Cosmochim. Acta 54, 413–424. https://doi.org/10.1016/S0341-8162(87)80006-1.

Berry, J., Bjorkman, O., 1980. Photosynthetic response and adaptation to temperature in higher plants. Annu. Rev. Plant Physiol. 31, 491–543. https://doi.org/10.1146/annurev.pp.31.060180.002423.

Boninsegna, J.A., Argollo, J., Aravena, J.C., Barichivich, J., Christie, D., Ferrero, M.E., Lara, A., Le Quesne, C., Luckman, B.H., Masiokas, M., Morales, M., Oliveira, J.M., Roig, F., Srur, A., Villalba, R., 2009. Dendroclimatological reconstructions in South America: a review. Palaeogeogr. Palaeoclimatol. Palaeoecol. 281, 210–228. https://doi.org/10.1016/j.palaeo.2009.07.020.

Briffa, K.R., 1995. Interpreting high-resolution proxy climate — the example of dendroclimatology. Anal. Clim. Var. 77–94. https://doi.org/10.1007/978-3-662-03744-7_5.

Brooks, J.R., Barnard, H.R., Coulombe, R., Mcdonnell, J.J., 2009. Ecohydrologic separation of water between trees and streams in a Mediterranean climate. Nat. Geosci. 3, 100–104. https://doi.org/10.1038/ngeo722.

Brumos, J., Robles, L.M., Yun, J., Vu, T.C., Jackson, S., Alonso, J.M., Stepanova, A.N., 2018. Local auxin biosynthesis is a key regulator of plant development. Dev. Cell 47, 1–13. https://doi.org/10.1016/j.devcel.2018.09.022.

Burns, B., 1991. The regeneration dynamics of Araucaria araucana.

Burns, B.R., 1993. Fire-induced dynamics of Araucaria araucana-Nothofagus antarctica forest in the southern Andes. J. Biogeogr. 20, 669–685. https://doi.org/10.2307/2845522.

Buttò, V., Deslauriers, A., Rossi, S., Rozenberg, P., Shishov, V., Morin, H., 2020. The role of plant hormones in tree-ring formation. Trees 34, 315–335. https://doi.org/10.1007/s00468-019-01940-4.

Cernusak, L.A., Barbour, M.M., Arndt, S.K., Cheesman, A.W., English, N.B., Feild, T.S., Helliker, B.R., Holloway-Phillips, M.M., Holtum, J.A.M., Kahmen, A., Mcinerney, F. A., Munksgaard, N.C., Simonin, K.A., Song, X., Stuart-Williams, H., West, J.B., Farquhar, G.D., 2016. Stable isotopes in leaf water of terrestrial plants. Plant Cell Environ. 39, 1087–1102. https://doi.org/10.1111/pce.12703.

Cheesman, A.W., Cernusak, L.A., 2016. Infidelity in the outback: climate signal recorded in Δ 18 O of leaf but not branch cellulose of eucalypts across an Australian aridity gradient. Tree Physiol. 37, 554–564. https://doi.org/10.1093/treephys/tpw121.

Coplen, T.B., 1996. New guidelines for reporting stable hydrogen, carbon, and oxygen isotope-ratio data. Geochim. Cosmochim. Acta 60, 3359–3360. https://doi.org/10.1016/0016-7037(96)00263-3.

Cuny, H.E., Rathgeber, C.B.K., 2014. Une synthèse sur le fonctionnement et la régulation des processus cellulaires de la formation du bois. Rev. For. Fr. 66, 761–777. https://doi.org/10.4267/2042/56750.

Davies, W.K.D., 2010. The Plant Hormones: Their Nature, Occurrence, and Functions. Plant hormones. Springer Netherlands, Dordr. 112, 1–15. https://doi.org/10.1007/978–94-017–9655-2_1.

Dawson, T.E., Ehleringer, J.R., 1993. Isotopic enrichment of water in the " woody " tissues of plants: implications for plant water source, water uptake, and other studies which use the stable isotopic composition of cellulose. Geochim. Cosmochim. Acta 57, 3487–3492. https://doi.org/10.1016/0016-7037(93)90554-A.

del Valle, H.F., 1998. Patagonian soils: a regional synthesis. Ecol. Austral 8, 103–123.

Díaz-Vaz, J.E., 1984. Araucaria araucana. Descripción Anatómica. BOSQUE 5, 117–118.

Dickmann, D.I., Kozlowski, T.T., 1970. Vegetative ReproductiveMobilization and Incorporation of Photoassimilated 14C by Growing Vegetative and Reproductive Tissues of Adult Pinus resinosa Ait. Trees Plant Physiol. 45, 284–288.

Dombrosky, J., 2020. A ~1000-year 13C Suess correction model for the study of past ecosystems. Holocene 30, 474–478. https://doi.org/10.1177/0959683619887416.

Dünser, K., Kleine-Vehn, J., 2015. Differential growth regulation in plants-the acid growth balloon theory. Curr. Opin. Plant Biol. 28, 55–59. https://doi.org/10.1016/j.pbi.2015.08.009.

Falcon-Lang, H.J., 2000. The relationship between leaf longevity and growth ring markedness in modern conifer woods and its implications for palaeoclimatic studies. Palaeogeogr. Palaeoclimatol. Palaeoecol. 160, 317–328. https://doi.org/10.1016/S0031-0182(00)00079-1.

Fu, P.L., Grießinger, J., Gebrekirstos, A., Fan, Z.X., Bräuning, A., 2017. Earlywood and latewood stable carbon and oxygen isotope variations in two pine species in Southwestern China during the recent decades. Front. Plant Sci. 7, 1–12. https://doi.org/10.3389/fpls.2016.02050.

Garreaud, R.D., Aceituno, P., 2007. Atmospheric Circulation and Climatic Variability. Oxford Univ. Press, pp. 45–59. https://doi.org/10.1093/oso/9780195313413.003.0010.

Garreaud, R.D., Vuille, M., Compagnucci, R., Marengo, J., 2009. Present-day South American climate. Palaeogeogr. Palaeoclimatol. Palaeoecol. 281, 180–195. https://doi.org/10.1016/j.palaeo.2007.10.032.

Garreaud, R.D., Lopez, P., Minvielle, M., Rojas, M., 2013. Large-scale control on the patagonian climate. J. Clim. 26, 215–231. https://doi.org/10.1175/JCLI-D-12-00001.1.

Glerum, C., 1980. Food sinks and food reserves of trees in temperate climates. N. Zealand J. For. Sci. 10, 176–185.

Gonfiantini, R., Gratziu, S., Tongiorgi, E., 1965. Oxygen isotopic composition of water in leaves. Isot. Radiat. Soil-Plant Nutr. Stud. 405–410.

Grießinger, J., Langhamer, L., Schneider, C., Saß, B.-l., Steger, D., Skvarca, P., Braun, M. H., Meier, W.J.-H., Srur, A.M., Hochreuther, P., 2018. Imprints of Climate Signals in a 204 Year δ 18 O Tree-Ring Record of Nothofagus pumilio From Perito Moreno Glacier, Southern Patagonia (50°S). Front. Earth Sci. 6, 1–17. https://doi.org/10.3389/feart.2018.00027.

Grossiord, C., Buckley, T.N., Cernusak, L.A., Novick, K.A., Poulter, B., Siegwolf, R.T.W., Sperry, J.S., Mcdowell, N.G., 2020. Tansley review Plant responses to rising vapor pressure deficit. New Phytol. 226, 1550–1566. https://doi.org/10.1111/nph.16485.

Hadad, M.A., Roig, F.A., 2016. Sex-related climate sensitivity of Araucaria araucana Patagonian forest-steppe ecotone. . Ecol. Manag. 362, 130–141. https://doi.org/10.1016/j.foreco.2015.11.049.

Hadad, M.A., Roig, F.A., Boninsegna, J.A., Patón, D., 2014. Age effects on the climatic signal in Araucaria araucana from xeric sites in Patagonia. Argent. Plant Ecol. Divers 1–9. https://doi.org/10.1080/17550874.2014.980350.

Hadad, M.A., González-Reyes, Á., Roig, F.A., Matskovsky, V., Cherubini, P., 2021. Tree-ring-based hydroclimatic reconstruction for the northwest Argentine Patagonia since 1055 CE and its teleconnection to large-scale atmospheric circulation. Glob. Planet. Change 202. https://doi.org/10.1016/j.gloplacha.2021.103496.

Harris, I., Osborn, T.J., Jones, P., Lister, D., 2020. Version 4 of the CRU TS monthly high-resolution gridded multivariate climate dataset. Sci. Data 7, 1–18. https://doi.org/10.1038/s41597-020-0453-3.

Helle, G., Schleser, G.H., 2004. Beyond CO_2-fixation by Rubisco - an interpretation of 13C/12C variations in tree rings from novel intra-seasonal studies on broad-leaf trees. Plant, Cell Environ. 27, 367–380. https://doi.org/10.1111/j.0016-8025.2003.01159.x.

Hersbach, H., Bell, B., Berrisford, P., Hirahara, S., Horányi, A., Muñoz-Sabater, J., Nicolas, J., Peubey, C., Radu, R., Schepers, D., Simmons, A., Soci, C., Abdalla, S., Abellan, X., Balsamo, G., Bechtold, P., Biavati, G., Bidlot, J., Bonavita, M., De Chiara, G., Dahlgren, P., Dee, D., Diamantakis, M., Dragani, R., Flemming, J., Forbes, R., Fuentes, M., Geer, A., Haimberger, L., Healy, S., Hogan, R.J., Hólm, E., Janisková, M., Keeley, S., Laloyaux, P., Lopez, P., Lupu, C., Radnoti, G., de Rosnay, P., Rozum, I., Vamborg, F., Villaume, S., Thépaut, J.N., 2020. The ERA5 global reanalysis. Q. J. R. Meteorol. Soc. 146, 1999–2049. https://doi.org/10.1002/qj.3803.

Holmes, R., 1983. Computer-assisted quality control in tree-ring dating and measurement. Tree-ring Bull. 43, 69–78.

Kagawa, A., Sugimoto, A., Maximov, T.C., 2006. Seasonal course of translocation, storage and remobilization of 13C pulse-labeled photoassimilate in naturally growing Larix gmelinii saplings. New Phytol. 171, 793–804. https://doi.org/10.1111/j.1469-8137.2006.01780.x.

Kimak, A., Leuenberger, M., 2015. Are carbohydrate storage strategies of trees traceable by early–latewood carbon isotope differences. Trees 29, 859–870. https://doi.org/10.1007/s00468-015-1167-6.

Knöller, K., Boettger, T., Weise, S.M., Gehre, M., 2005. Carbon isotope analyses of cellulose using two different on-line techniques (elemental analysis and high-temperature pyrolysis) - a comparison. Rapid Commun. Mass Spectrom. 19, 343–348. https://doi.org/10.1002/rcm.1793.

Kozlowski, T.T., 1992. Carbohydrate sources and sinks in woody plants. Bot. Rev. 58, 107–222. https://doi.org/10.1007/BF02858600.

Kress, A., Young, G.H.F., Saurer, M., Loader, N.J., Siegwolf, R.T.W., McCarroll, D., 2009. Stable isotope coherence in the earlywood and latewood of tree-line conifers. Chem. Geol. 268, 52–57. https://doi.org/10.1016/j.chemgeo.2009.07.008.

Lara, A., Villalba, R., Urrutia-Jalabert, R., González-Reyes, A., Aravena, J.C., Luckman, B. H., Cuq, E., Rodríguez, C., Wolodarsky-Franke, A., 2020. +A 5680-year tree-ring temperature record for southern South America. Quat. Sci. Rev. 228, 1–14. https://doi.org/10.1016/j.quascirev.2019.106087.

Lavergne, A., 2016. Evaluation of tree-ring archive as paleoclimatic tracer in northern Patagonia.

Lavergne, A., Daux, V., Villalba, R., Pierre, M., Stievenard, M., Srur, A.M., Vimeux, F., 2016. Are the δ18O of F. cupressoides and N. pumilio promising proxies for climate reconstructions in northern Patagonia? J. Geophys. Res. Biogeosci. 121, 767–776. https://doi.org/10.1002/2015JG003260.

Lavergne, A., Daux, V., Villalba, R., Pierre, M., Stievenard, M., Srur, A.M., 2017a. Improvement of isotope-based climate reconstructions in Patagonia through a better understanding of climate influences on isotopic fractionation in tree rings. Earth Planet. Sci. Lett. 1, 1–9. https://doi.org/10.1016/j.epsl.2016.11.045.

Lavergne, A., Gennaretti, F., Risi, C., Daux, V., Boucher, E., Savard, M.M., Naulier, M., Villalba, R., Bégin, C., Guiot, J., 2017b. Modelling tree ring cellulose δ 18 O variations in two temperature-sensitive tree species from North and South America. Clim 13, 1515–1526. https://doi.org/10.5194/cp-13-1515-2017.

Lavergne, A., Daux, V., Pierre, M., Stievenard, M., Srur, A., Villalba, R., 2018. Past summer temperatures inferred from dendrochronological records of fitzroya cupressoides on the Eastern Slope of the Northern Patagonian Andes. J. Geophys. Res. Biogeosci. https://doi.org/10.1002/2017JG003989.

Le Quesne, C., Stahle, D.W., Cleaveland, M.K., Therrell, M.D., Aravena, J.C., Barichivich, J., 2006. Ancient Austrocedrus tree-ring chronologies used to reconstruct central Chile precipitation variability from A.D. 1200 to 2000. J. Clim. 19, 5731–5744. https://doi.org/10.1175/JCLI3935.1.

Leavitt, S.W., Danzer, S.R., 1993. Method for batch processing small wood samples to holocellulose for stable-carbon isotope analysis. Anal. Chem. 65, 87–89. https://doi.org/10.1021/ac00049a017.

Ljung, K., Hull, A.K., Celenza, J., Yamada, M., Estelle, M., Normanly, J., Sandberg, G., 2005. Sites and regulation of auxin biosynthesis in arabidopsis roots. Plant Cell 17, 1090–1104. https://doi.org/10.1105/tpc.104.029272.

Majda, M., Robert, S., 2018. The role of auxin in cell wall expansion. Int. J. Mol. Sci. 19, 1–21. https://doi.org/10.3390/ijms19040951.

Meier, W.J., 2019. Past and recent climate variability and glacier fluctuations across the Southern Patagonian Andes.

Morales, M.S., Christie, D.A., Villalba, R., Argollo, J., Pacajes, J., Silva, J.S., Alvarez, C. A., Llancabure, J.C., Gamboa, C.C.S., 2012. Precipitation changes in the South American Altiplano since 1300 AD reconstructed by tree-rings. Clim 8, 653–666. https://doi.org/10.5194/cp-8-653-2012.

Mott, K.A., Woodrow, I.E., 2000. Modelling the role of Rubisco activase in limiting non-steady-state photosynthesis. J. Exp. Bot. 51, 399–406. https://doi.org/10.1093/jexbot/51.suppl_1.399.

Mundo, I.A., Jun, F.A.R., Villalba, R., Kitzberger, T., Barrera, M.D., 2012. Araucaria araucana tree-ring chronologies in Argentina: spatial growth variations and climate influences. Trees 26, 443–458. https://doi.org/10.1007/s00468-011-0605-3.

Muñoz, A.A., Barichivich, J., Christie, A.D., Dorigo, W., Sauchyn, D., Gonzalez-Reyes, A., Villalba, R., Lara, A., Riquelme, N., Gonzalez, M.E., 2013. Patterns and drivers of Araucaria araucana forest growth along a biophysical gradient in the northern Patagonian Andes: linking tree rings with s. Austral Ecol. 12 https://doi.org/10.1111/aec.12054.

Puchi, P.F., Camarero, J.J., Battipaglia, G., Carrer, M., 2021. Retrospective analysis of wood anatomical traits and tree-ring isotopes suggests site-specific mechanisms triggering Araucaria araucana drought-induced dieback. Glob. Chang. Biol. 27, 6394–6408. https://doi.org/10.1111/gcb.15881.

Rathgeber, C.B.K., 2020. Ecophysiology of Tree-ring Formation: Concepts, Methods and Applications.

Rathgeber, C.B.K., Cuny, H.E., Fonti, P., 2016. Biological basis of tree-ring formation: a crash course. Front. Plant Sci. 7, 1–7. https://doi.org/10.3389/fpls.2016.00734.

Requena-Rojas, E.J., Morales, M., Villalba, R., 2020. Dendroclimatological assessment of Polylepis rodolfo-vasquezii: a novel Polylepis species in the Peru highlands. Dendrochronologia 62, 125722. https://doi.org/10.1016/j.dendro.2020.125722.

Roden, J.S., Farquhar, G.D., 2012. A controlled test of the dual-isotope approach for the interpretation of stable carbon and oxygen isotope ratio variation in tree rings. Tree Physiol. 32, 490–503. https://doi.org/10.1093/treephys/tps019.

Rodriguez-Caton, M., Andreu-Hayles, L., Morales, M.S., Daux, V., Christie, D.A., Coopman, R.E., Alvarez, C., Rao, M.P., Aliste, D., Flores, F., Villalba, R., 2021. Different climate sensitivity for radial growth, but uniform for tree-ring stable isotopes along an aridity gradient in Polylepis tarapacana, the world's highest elevation tree-species. Tree Physiol. https://doi.org/10.1093/treephys/tpab021.

Roig, F.A., Siegwolf, R., Boninsegna, J.A., 2006. Stable oxygen isotopes (δ18O) in Austrocedrus chilensis tree rings reflect climate variability in northwestern Patagonia, Argentina. Int. J. Biometeorol. 51, 97–105. https://doi.org/10.1007/s00484-006-0049-4.

Rothfuss, Y., Javaux, M., 2017. Reviews and syntheses: isotopic approaches to quantify root water uptake: a review and comparison of methods. Biogeosciences 14, 2199–2224. https://doi.org/10.5194/bg-14-2199-2017.

Running, S.W., 1976. Environmental control of leaf water conductance in conifers. Can. J. For. Res. 6, 104–112. https://doi.org/10.1139/x76-013.

Scheidegger, Y., Saurer, M., Bahn, M., Siegwolf, R., 2000. Linking stable oxygen and carbon isotopes with stomatal conductance and photosynthetic capacity: a conceptual model. Oecologia 125, 350–357. https://doi.org/10.1007/s004420000466.

Scheuring, D., Löfke, C., Krüger, F., Kittelmann, M., Eisa, A., Hughes, L., Smith, R.S., Hawes, C., Schumacher, K., Kleine-Vehn, J., 2016. Actin-dependent vacuolar occupancy of the cell determines auxin-induced growth repression. Proc. Natl. Acad. Sci. U. S. A. 113, 452–457. https://doi.org/10.1073/pnas.1517445113.

Schulman, E., 1956. Dendroclimatic changes in semiarid America. University of Arizona Press, Tucson.

Sprenger, M., Leistert, H., Gimbel, K., Weiler, M., 2016. Illuminating hydrological processes at the soil-vegetation- atmosphere interface with water stable isotopes. Rev. Geophys. 54, 674–704. https://doi.org/10.1002/2015RG000515.

Stokes, M.A., Smiley, T.L., 1968. An Introduction to Tree-Ring Dating.

Szejner, P., Clute, T., Anderson, E., Evans, M.N., Hu, J., 2020. Reduction in lumen area is associated with the δ18O exchange between sugars and source water during cellulose synthesis. New Phytol. 226, 1583–1593. https://doi.org/10.1111/nph.16484.

Taiz, L., Zeiger, E., 2002. Plant physiology (Third Edition), Science progress. Sinauer Associates, Inc., Publishers, Sunderland. https://doi.org/10.1017/9781108486392.

Teten, O., 1930. Über einige meteorologische Begriffe. Z. für Geophys 6, 297–309.

Tognetti, R., Lombardi, F., Lasserre, B., Cherubini, P., Marchetti, M., 2014. Tree-ring stable isotopes reveal twentieth-century increases in water-use efficiency of fagus sylvatica and Nothofagus spp. in Italian and Chilean Mountains. PLoS One 9, 1–16. https://doi.org/10.1371/journal.pone.0113136.

Tortorelli, L.A., 1956. Maderas y bosques argentinos. Editorial Acme. Buenos Aires.

Urrutia-Jalabert, R., Malhi, Y., Barichivich, J., Lara, A., Delgado-Huertas, A., Rodríguez, C.G., Cuq, E., 2015c. Increased water use efficiency but contrasting tree growth patterns in Fitzroya cupressoides forests of southern Chile during recent decades. J. Geophys. Res. Biogeosci. 120, 2505–2524. https://doi.org/10.1002/2015JG003098.

Veblen, T.T., 1982. Regeneration patterns in Araucaria araucana forests in Chile. J. Biogeogr. 9, 11. https://doi.org/10.2307/2844727.

Veblen, T.T., Burns, B.R., Kitzberger, T., Lara, A., Villalba, R., 1995. The ecology of the conifers of Southern South America. Ecol. South. Conifers 120–155.

Vicente-Serrano, S.M., Beguería, S., López-Moreno, J.I., 2010. A multiscalar drought index sensitive to global warming: the standardized precipitation evapotranspiration index. J. Clim. 23, 1696–1718. https://doi.org/10.1175/2009JCLI2909.1.

Villalba, R., 1990. Climatic fluctuations in Northern Patagonia during the last 1000 records years as inferred from tree-ring records. Quat. Res. 34, 346–360.

Villalba, R., 1995. Geograpgical variations in tree-growth responses to climate in the Southern Andes. Cambios Cuatern. En. América Del. Sur 307–317.

Villalba, R., Boninsegna, J.A., Lara, A., Veblen, T.T., Roig, F.A., Aravena, J.C., Ripalta, A., 1996. Interdecadal climatic variations in millenial temperature reconstructions from southern South America. In: Jones, P.D., Bradley, R.S., Jouzel, J. (Eds.), Clim. Var. Forcing Mech. Last 2000 years NATO ASI Ser, 141, pp. 161–189. https://doi.org/10.1007/978-3-642-61113-1.

Villalba, R., Cook, E.R., Jacoby, G.C., D'Arrigo, R.D., Veblen, T.T., Jones, P.D., 1998. Tree-ring based reconstructions of northern Patagonia precipitation since AD 1600. Holocene 8, 659–674. https://doi.org/10.1191/095968398669095576.

Villalba, R., Lara, A., Boninsegna, J.A., Masiokas, M., Delgado, S., Aravena, J.C., Roig, F. A., Schmelter, A., Wolodarsky-Franke, A., Ripalta, A., 2003. Large-scale temperature changes across the Southern Andes: 20th Century variations in the context of the past 400 years. Clim. Change 97, 131–141. https://doi.org/10.1023/A.

Villalba, R., Lara, A., Masiokas, M.H., Urrutia, R., Luckman, B.H., Marshall, G.J., Mundo, I.A., Christie, D.A., Cook, E.R., Neukom, R., Allen, K., Fenwick, P., Boninsegna, J.A., Srur, A.M., Morales, M.S., Araneo, D., Palmer, J.G., Cuq, E., Aravena, J.C., Holz, A., LeQuesne, C., 2012. Unusual Southern Hemisphere tree growth patterns induced by changes in the Southern Annular Mode. Nat. Geosci. 5, 793–798. https://doi.org/10.1038/ngeo1613.

Wigley, T.M.L., Briffa, K.R., Jones, P.D., 1984. On the average value of correlated time series, with applications in dendroclimatology and hydrometeorology. J. Clim. Appl.

Meteorol. 23, 201–213. https://doi.org/10.1175/1520-0450(1984)023<0201:OTAVOC>2.0.CO;2.
Woodley, E.J., Loader, N.J., McCarroll, D., Young, G.H.F., Robertson, I., Heaton, T.H.E., Gagen, M.H., Warham, J.O., 2012. High-temperature pyrolysis/gas chromatography/isotope ratio mass spectrometry: Simultaneous measurement of the stable isotopes of oxygen and carbon in cellulose. Rapid Commun. Mass Spectrom. 26, 109–114. https://doi.org/10.1002/rcm.5302.
Yamaguchi, D.K., 1991. A simple method for cross-dating increment cores from living trees. Can. J. For. Res. 414–416.
Zhao, Y., 2010. Auxin biosynthesis and its role in plant development. Annu. Rev. Plant Biol. 61, 49–64. https://doi.org/10.1146/annurev-arplant-042809-112308.
Zhong, R., Ye, Z.-H., 2009. Secondary cell walls. Encycl. Life Sci. https://doi.org/10.1002/9780470015902.a0021256.
Zweifel, R., Sterck, F., 2018. A conceptual tree model explaining legacy effects on stem growth. Front. For. Glob. Chang 1, 1–9. https://doi.org/10.3389/ffgc.2018.00009.